

Dissipation at the core-mantle boundary on a small-scale topography

J. L. Le Mouél,¹ C. Narteau,² M. Greff-Lefftz,¹ and M. Holschneider³

Received 23 May 2005; revised 13 October 2005; accepted 27 December 2005; published 27 April 2006.

[1] The parameters of the nutations are now known with a good accuracy, and the theory accounts for most of their values. Dissipative friction at the core-mantle boundary (CMB) and at the inner core boundary is an important ingredient of the theory. Up to now, viscous coupling at a smooth interface and electromagnetic coupling have been considered. In some cases they appear hardly strong enough to account for the observations. We advocate here that the CMB has a small-scale roughness and estimate the dissipation resulting from the interaction of the fluid core motion with this topography. We conclude that it might be significant.

Citation: Le Mouél, J. L., C. Narteau, M. Greff-Lefftz, and M. Holschneider (2006), Dissipation at the core-mantle boundary on a small-scale topography, *J. Geophys. Res.*, *111*, B04413, doi:10.1029/2005JB003846.

1. Introduction

[2] The question of the dissipation at the core-mantle boundary (CMB) (and also at the inner core boundary, but we focus here on the CMB) is of some importance in global geodynamics [e.g., *Greff-Lefftz and Legros, 1999*] but cannot be said to be fully understood at this time. This dissipation can be estimated from the estimates of the coefficients of the nutation series. As a matter of fact, the main properties of the Earth that affect its rotational response to a set of periodic gravitational luni-solar torques are the presence of the fluid core and solid inner core, the interactions occurring at the core boundaries (CMB and ICB), the rheological properties of the mantle (including anelasticity), and the presence of the oceans. *Mathews et al. [2002]* model theoretical values from the nutation series, and, among the geophysical results they obtain from their fit between observations and theoretical values, are estimates of the dynamic ellipticity of the Earth and of the fluid core and of the two complex coupling constants related to the dissipative power at the CMB and at the ICB.

[3] *Herring et al. [2002]* estimate the coefficients of the nutation series with standard deviations ranging from 5 microseconds of arc (μs) for the terms with periods <400 days to 38 μs for the longest-period terms. The deviations between the VLBI estimates of the amplitudes of terms in the nutations series and the theoretical values from the *Mathews et al. [2002]* nutation series are at the level of the standard deviation for nutational terms with periods <400 days. In particular, the residuals in the out of

phase amplitudes of the retrograde 18.6 year and annual nutations, which had long remained at 0.5 milliseconds of arc (mas), are now also reduced to the level of the uncertainties in the observational estimates. The largest remaining discrepancy is that in the out of phase prograde 18.6 year nutation (of 72 μs).

[4] Dissipation is due to relative motions of the fluid core with respect to the mantle. As the fluid core is viscous, and the lower mantle conducting, resistive torques between the core and the mantle result from those relative motions, and power is dissipated. The amount of power dissipated, either due to core viscosity or to electromagnetic coupling, has been estimated for long. It depends on the value of the viscosity and the conductivity model of the mantle. It has been shown that conductivity models with a weak conductivity value throughout the mantle could not account for the observed values of some nutation. *Buffett et al. [2002]* called for the presence of a thin conducting layer at the base of the mantle with a total conductance of 10^8 S, and a RMS radial magnetic field at the CMB of about 6.9 gauss, for simple magnetic field configurations. The total conductance of weak conductivity models [*Shankland et al., 1993*], which do not include such a higher conductivity thin layer, is 10^7 S. However, the existence of a high-conductivity layer is not really supported by independent clues [*Poirier et al., 1998*]. Let us also point out that *Mathews et al. [2002]* did not take into account the viscosity of the fluid core; this viscosity can change the coupling constants. More important, the negative sign of the imaginary part of the Chandler frequency [*Mathews et al., 2002, Table 3a*] means that for the considered model of the Earth, the electromagnetic torque leads to the excitation of the wobble, not to the dissipation of energy. For these reasons, search of other sources of the dissipation at the CMB and at the ICB is very important.

[5] In a recent paper [*Narteau et al., 2001*], we advocated the presence at the CMB of a short-scale topography, or roughness, resulting from a dynamical physico-chemical equilibrium at this boundary. We briefly present the results

¹Laboratoire de Géomagnétisme, Institut de Physique du Globe de Paris, Paris, France.

²Laboratoire de Dynamique des Systèmes Géologiques, Institut de Physique du Globe de Paris, Paris, France.

³Institute of Applied and Industrial Mathematics, Universität Potsdam, Potsdam, Germany.

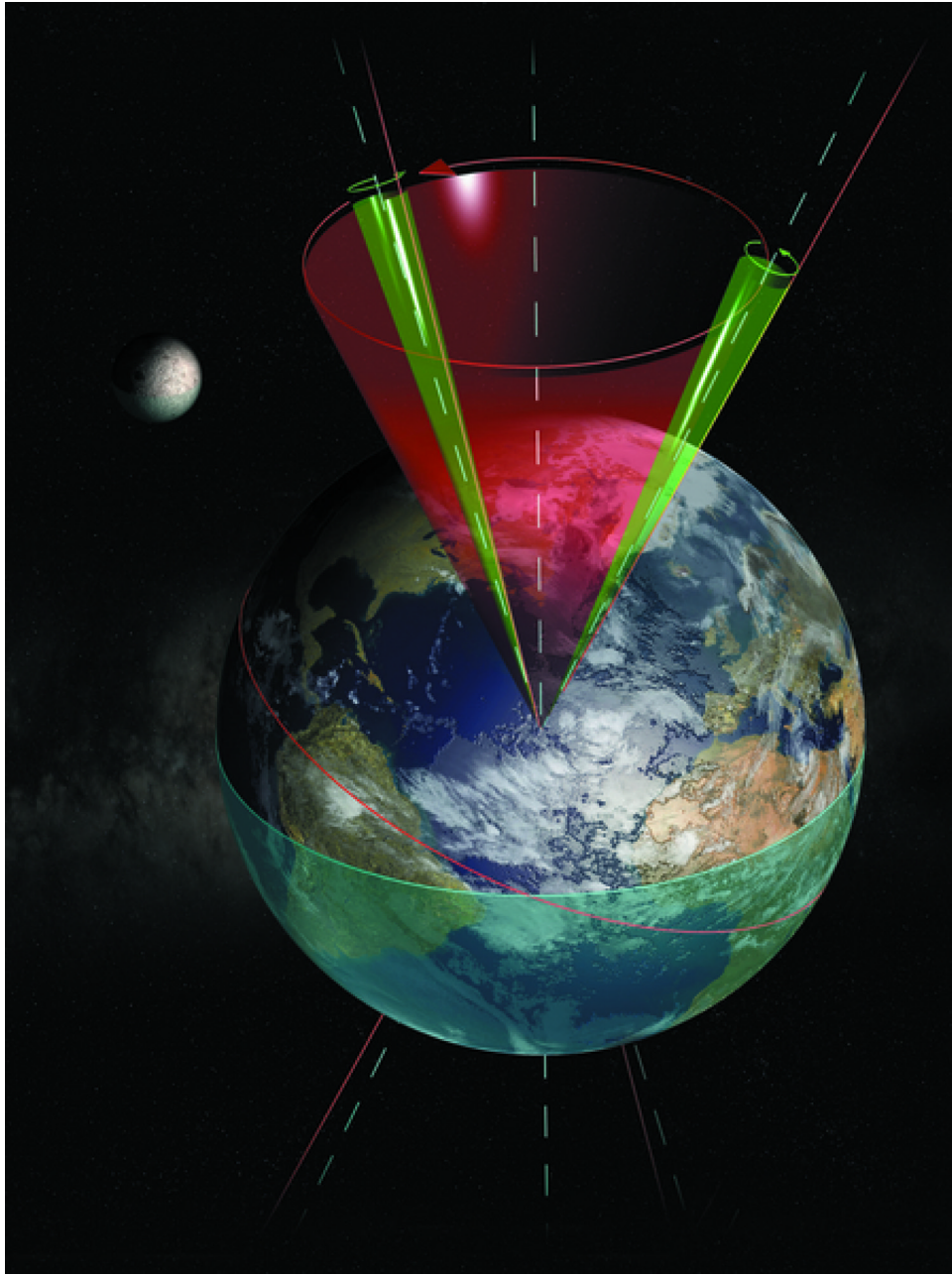


Figure 1. Precession and nutation of the Earth's spin axis. The precession cone (red) and two nutation cones (green) are highlighted (from Greff [2004] with permission from *Pour la Science*).

of an extension of this model (essentially from two to three dimensions) and show that the interaction between the core fluid flow and this roughness may also significantly contribute to the required amount of dissipation. Also, we discuss some consequences.

2. Poincaré Flows Related to Precession and Nutation

[6] A number of detailed and complete papers have been devoted to these flows [e.g., *Poincaré*, 1910; *Stewartson and Roberts*, 1963; *Roberts and Stewartson*, 1965; *Busse*, 1968; *Stacey*, 1973; *Toomre*, 1974; *Loper*, 1975; *Rochester*, 1976; *Sasao et al.*, 1977; *Kerswell*, 1993; *Vanyo*, 1991;

Vanyo et al., 1995; *Néron de Surgy and Laskar*, 1997; *Pais et al.*, 1999; *Tilgner*, 1999; *Pais and Le Mouél*, 2001; *Noir et al.*, 2001]. We content ourselves here to give a very short and simplified account of these motions, and the few formulas necessary for the following.

[7] Precession and nutation of the Earth's spin axis are generated by the action of the degree 2 tesseral term of the luni-solar gravitational potential on the Earth's equatorial bulge [e.g., *Bretagnon and Capitaine*, 1997]. Precession, the Earth's rotation axis describes a cone of 23.5° half angle in 26000 years, is due to the constant part (κ_1) of the luni-solar torque. In addition, as the Moon and Sun orbits with respect to the Earth present various periodic perturbations, the luni-solar torque presents the same periodicities and

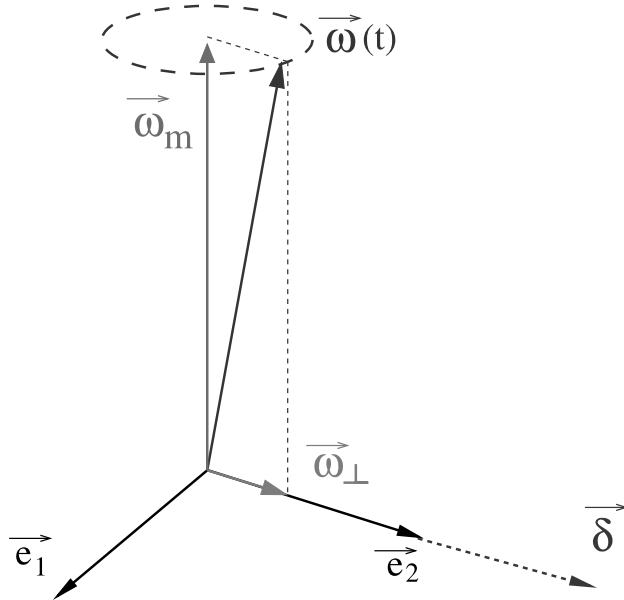


Figure 2. Annual retrograde nutation. The \mathbf{e}_1 and \mathbf{e}_2 are in the Earth's equatorial plane rotating with ω_{\perp} , and δ is the angular rotation of the core with respect to the mantle in the $(\mathbf{e}_1, \mathbf{e}_2, \omega)$ frame.

generates small motions of the Earth's rotation axis around its mean direction which itself precesses on the precession cones (Figure 1). Let us consider a single nutation of angular frequency $\varepsilon\omega$, $|\varepsilon| \ll 1$, in absolute space. The spin axis ω describes a small cone around ω_m , the mean value of the spin, over a period $2\pi/|\varepsilon\omega| = \tau$, ω_m itself precessing on the precession cone. In other words, ω has an equatorial component ω_{\perp} in the plane (ω_m, ω) , rotating with period τ , $\omega_{\perp} = \omega_{\perp} \mathbf{e}_2$ (Figure 2). A quasi-solid rotation δ of the core with respect to the mantle results, around the same axis \mathbf{e}_2 (approximately). It happens that δ is amplified with respect to ω_{\perp} :

$$\delta = \omega_{\perp} f.$$

The amplification factor f would be simply $1/(e + \varepsilon)$ in the case of a rigid mantle, $e = (c - a)/a$, c and a being the polar and equatorial semiaxes, respectively, of the ellipsoidal core. However, the mantle elasticity has to be taken into account. It comes [Greff-Leffitz and Legros, 1999]

$$\delta = \omega_{\perp} \frac{1 - (q_0/2\alpha)h_c}{e + \varepsilon - (q_0 h_c^1/2)},$$

where $h_c = 1.137$ and $h_c^1 = 0.356$ are Love numbers (computed for a stratified PREM model) characterizing the CMB deformation induced by the mantle and the core rotational potentials, α is the dynamical flattening of the core and

$$q_0 = \frac{\omega^2 R}{g_0} = \frac{1}{289.9}$$

is the geodetic constant (R the Earth's mean radius, g_0 the gravity at the Earth's surface). In the case of the annual

retrograde Ψ_1 tidal wave, $\varepsilon = -(1/366.25)$, and it comes $f = -590$.

[8] A friction torque results

$$\Gamma = -\kappa\delta - \kappa'(\mathbf{e}_1 \times \mathbf{e}_2) \times \delta$$

or, using complex notations,

$$\Gamma_1 + i\Gamma_2 = -(\kappa + i\kappa')(\delta_1 + i\delta_2)$$

and a power dissipated by friction:

$$\mathcal{P} = \kappa\delta^2$$

$\delta = \sqrt{\delta_1^2 + \delta_2^2}$, κ is a friction coefficient

$$\kappa = \kappa_v + \kappa_m$$

sum of a viscous coefficient and an electromagnetic coefficient. The expression of the viscous coefficient has been computed by Roberts [1965], Busse [1968], and Loper [1975]:

$$\kappa_v = 2.62C_n \frac{\sqrt{\nu^*\omega}}{R_c}$$

C_n is the axial inertia momentum of the core ($C_n \approx 8.9 \times 10^{36} \text{ kg m}^2$), R_c is the mean core radius ($R_c \approx 3.5 \times 10^6 \text{ m}$), and ν^* is the core liquid kinematic viscosity. For $\nu^* \approx 10^{-7} \text{ m}^2 \text{ s}^{-1}$, $\kappa_v = 0.18 \times 10^{26} \text{ kg m}^2 \text{ s}^{-1}$. This value is an estimate of the molecular viscosity of the liquid core, computed from general considerations on the transport properties of iron in the core pressure and temperature conditions. In other questions, values of an effective, e.g., turbulent, viscosity are considered, spanning orders of magnitude.

[9] The constant of electromagnetic coupling κ_m has been computed by MacDonald and Ness [1961] in a plane geometry and by Buffett [1992] in a spherical geometry for a constant conductivity σ_m of the lower mantle and an insulating upper mantle (the skin depth for a daily frequency is smaller than the thickness of the lower conductive layer). Considering the field dipolar and $\sigma_c \gg \sigma_m$:

$$\kappa_m = \frac{32\pi}{15} \frac{R^6}{R_c^2} (g_1^0)^2 \sqrt{\frac{2\sigma_m}{\mu\omega}}$$

where R is the mean Earth's radius, σ_m is the electrical conductivity of the lower mantle (σ_c is the core conductivity), g_1^0 is the axial dipolar Gauss coefficient, and μ is the permeability of void ($\mu = 4\pi \cdot 10^{-7}$). Taking $g_1^0 = 3 \times 10^{-5} \text{ T}$ and $\sigma_m = 10 (\Omega \text{ m})^{-1}$ (weak conductivity model, but see section 3), we obtain $\kappa_m = 0.15 \times 10^{26} \text{ kg m}^2 \text{ s}^{-1}$. With these values of the parameters, κ_v and κ_m have the same order of magnitude.

[10] The daily angular frequency ω enters both the expressions of κ_v and κ_m for the following reason; δ is moving slowly in the absolute space ($2\pi/\varepsilon\omega \gg 1$ day), so it is moving with a nearly diurnal frequency with respect to the rotating Earth. Whereas the motion of the core with respect to the mantle is a simple rotation in the frame $(\mathbf{e}_1, \mathbf{e}_2,$

e_3) of Figure 2, the liquid flow field as viewed from the rotating mantle shows a periodic oscillation with a period close to 1 day with a complex structure (see, e.g., *Pais and Le Mouël* [2001] for an illustration of this flow).

3. Annual Retrograde Nutation

[11] The annual retrograde nutation is generated by the Ψ_1 tidal wave whose period in an absolute frame is $-\varepsilon\omega$, and $-\omega(1 - \varepsilon)$ in a frame linked to the mantle [e.g., *Bretagnon and Capitaine*, 1997; *Greff-Lefftz and Legros*, 1999]. VLBI observations provide a fairly accurate determination of the annual retrograde nutation parameters, i.e., the amplitude of the in-phase and out-of-phase components of ω_{\perp} (the phase being reckoned from the forcing tidal term). As indicated in section 1, *Buffett* [1992] and *Buffett et al.* [2002] showed that the measured amplitude of the out of phase component requires a very efficient magnetic torque acting at the CMB to correct for the discrepancy between the observed and the theoretical curves which remains after taking into account the ocean tide and mantle anelasticity.

[12] More precisely, in addition to considering multipole terms of the magnetic field at the CMB, Buffet proposed an enhanced conductivity at the bottom of the mantle, which he modeled as a 500 m layer with a conductivity of 5×10^5 ($\Omega \text{ m}$)⁻¹, the conductivity of the core. However, the existence of such a layer has been discussed by *Poirier and Le Mouël* [1992], *Le Mouël et al.* [1997], and *Poirier et al.* [1998]. They argued that neither partial melting nor infiltration of the lower mantle by core iron could account for such an enhanced conductivity, and concluded in favor of a low conductivity ($\sigma < 10$ ($\Omega \text{ m}$)⁻¹) throughout the mantle. More recently, *Buffett et al.* [2000] proposed, instead of this high-conductivity layer in the lower mantle, a thin layer of silicate sediment which accumulates at the top of the core as the Earth cools and could have the required conductance of 1.7×10^8 S. The existence of such a layer of silicate sediment is not firmly established, neither its coupling with the mantle well understood.

[13] Before moving to the very subject of the present paper, let us recall the power dissipated at the CMB by the motion linked to the retrograde annual nutation (Ψ_1), $\kappa\delta^2$, for both the weak conductivity model ($\sigma = 10$ ($\Omega \text{ m}$)⁻¹ throughout the 2000 km of the lower mantle) and the high conductivity model of Buffet [*Greff-Lefftz and Legros*, 1999, Table 1], assuming first an axial dipolar magnetic field (with a Gauss coefficient $g_1^0 = 3 \times 10^{-5}$ T):

$$\text{weak conductivity} \quad \mathcal{P} = 2.7 \times 10^4 \text{ W}$$

$$\text{strong conductivity} \quad \mathcal{P} = 6.9 \times 10^5 \text{ W.}$$

[14] The magnetic power dissipated at the CMB varies as the square of the amplitude of the magnetic field. Thus these values may be increased if assuming a more complex magnetic field [*Buffett et al.*, 2002]. Nevertheless, they are still smaller than 4.7×10^6 W, the dissipated power estimated from the frictional constants determined by *Mathews et al.* [2002]. So there is room for looking at alternative or complementary mechanisms.

[15] We will argue that a power of the order of 10^6 W might be provided by the friction of the Poincaré flow on a small-

scale topography likely to exist at the CMB, adding, as announced in the introduction, another source of dissipation.

4. Small-Scale Topography (Roughness) of the CMB

[16] *Narteau et al.* [2001] argued that there may be a small roughness at the CMB, invisible to seismology. There is a striking contrast between the mantle and the core; the mantle is rocky, composed mostly of crystalline silicate perovskite and magnesiowüstite with a density of 5600 kg m^{-3} near the core-mantle boundary, whereas the core consists of a dense (10^4 kg m^{-3}) molten iron alloy with a small viscosity. The CMB is expected to be the seat of physical-chemical interactions between core and mantle [*Le Mouël et al.*, 1997]. The hot liquid core can corrode the overlying mantle, preferentially dissolving the silicates and oxides along the grain boundaries and infiltrating upward into the mantle by capillarity [*Knittle and Jeanloz*, 1989; *Poirier and Le Mouël*, 1992]. The thickness of the infiltrated layer cannot exceed a few meters, which corresponds to the height for which the weight of the intergranular thin sheets of dense liquid is equilibrated by the interfacial tension between crystals and molten iron [*Le Mouël et al.*, 1997]. On that scale the grains of the crystalline mantle surrounded by liquid can be loosened, float at the top of the core, and go on dissolving in the core fluid undersaturated in the light elements constitutive of mantle minerals (mostly oxygen and silicon). The core fluid is consequently enriched in these light elements, and may become locally saturated; the light elements may then diffuse from the saturated toward the still unsaturated fluid. The saturated alloy, enriched in elements lighter than the bulk of the core fluid, is buoyant and tends to float upward near the CMB. Two competing processes take place at the CMB: crystals of the mantle are loosened and dissolved in the fluid, while crystalline matter is redeposited at other places. The small-scale roughness of the CMB is therefore due to the dynamic equilibrium between dissolution and redeposition. This can be compared to what happens on the atomic scale in the case of a crystal surface in equilibrium with a saturated solution or saturating vapor: atoms are continually dissolved (evaporated) and deposited (condensed) on the surface, imparting to it a roughness on the atomic scale.

[17] Thus the CMB does not move upward or downward but may acquire a roughness on scales larger than the grain size of the mantle material, superimposed to the topography at the scale of hundreds to thousands kilometers, due to mantle convection.

[18] *Narteau et al.* [2001] applied a cellular automaton method to model the short-scale topography according to the principles recalled above. The transition from a two-dimensional (2-D) to a 3-D model has been implemented recently to insure that the properties of the calculated topography remain. Cubic cells, with a characteristic length scale of the size of grains of the mantle material, can be in one of three states corresponding to mantle silicate or oxide, core fluid saturated in light element, and unsaturated core fluid, respectively. The model depends essentially on three parameters: the grain size d , the diffusion coefficient D of the light element in the liquid alloy, and the difference between the concentration of light element at saturation, f_{sat} , and the concentration f_0 in the unsaturated alloy (the bulk of

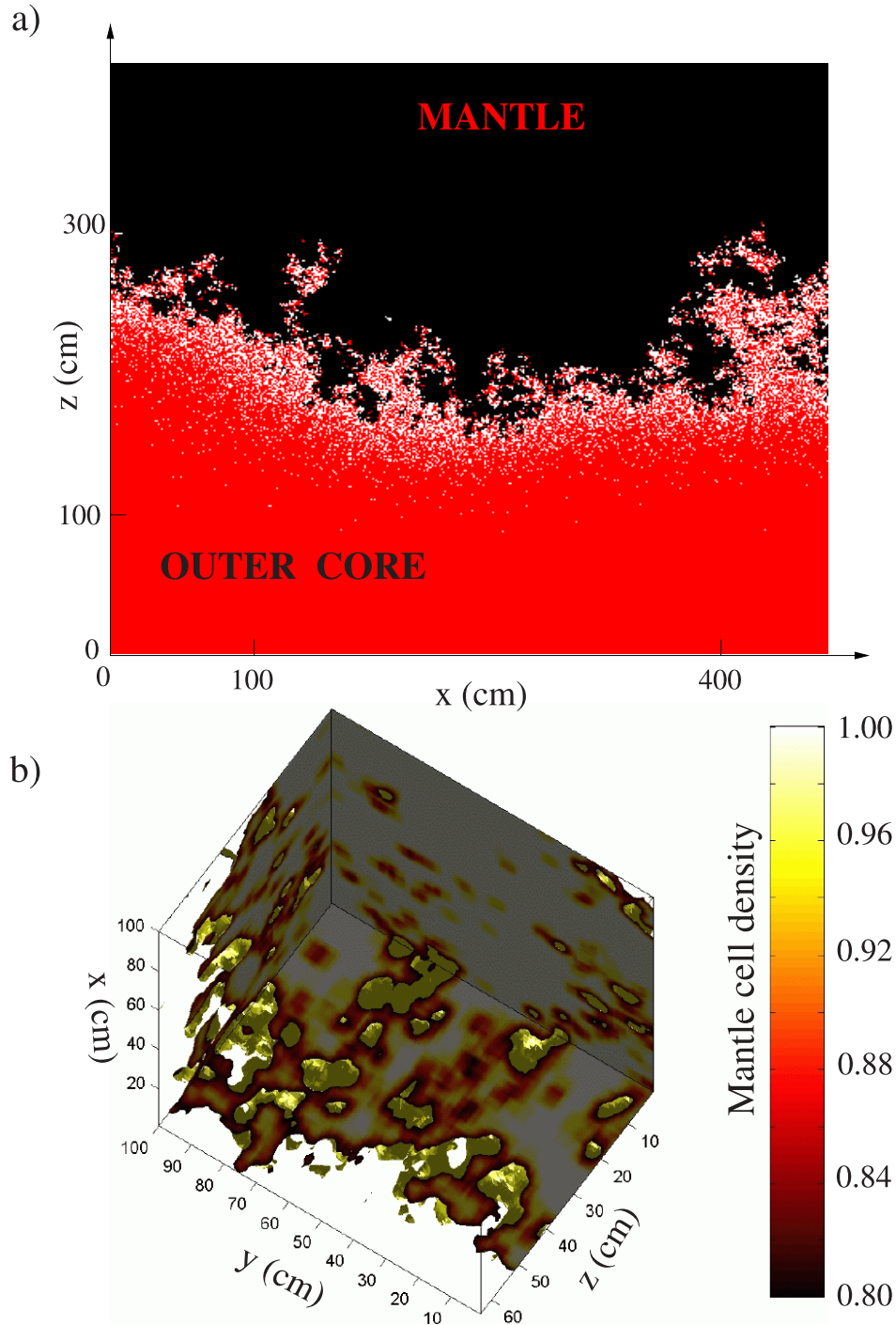


Figure 3. (a) Vertical section of the cellular automaton on a meter scale (red, white, and black are nonsaturated liquid iron, saturated liquid iron and solid silicate, respectively). (b) Density of mantle cells in a 3-D representation (this density is estimated locally within a $5 \times 5 \times 5$ windows).

the core). Realizations of the model have been computed for $d = 1$ cm, $D = 3 \times 10^{-9}$ m² s⁻¹ and different values of f_{sat} ranging from $1.25f_0$ to $3f_0$ [Narteau *et al.*, 2001]. No constraint on the scale of the topography is given a priori.

[19] For $f_{\text{sat}} = 2f_0$, Figure 3 shows a vertical section of cells (Figure 3a) and the density of mantle cells (Figure 3b) at the meter scale of the modelled CMB. Representations at larger scales are given by Narteau *et al.* [2001]. Characteristic length scales of tens of meters have been observed in 2-D

computations. In the 3-D computation, $h_s(i, j, t)$ being the ordinates of the boundary between the solid mantle and the saturated liquid alloy (i and j are counted in units of d , the grain size, t is time), we define the roughness of the CMB as

$$R_u(t) = \frac{1}{L} \sqrt{\sum_{i=1}^L \sum_{j=1}^L [h_s(i, j, t) - \bar{h}_s(i, j, t)]^2}, \quad (1)$$

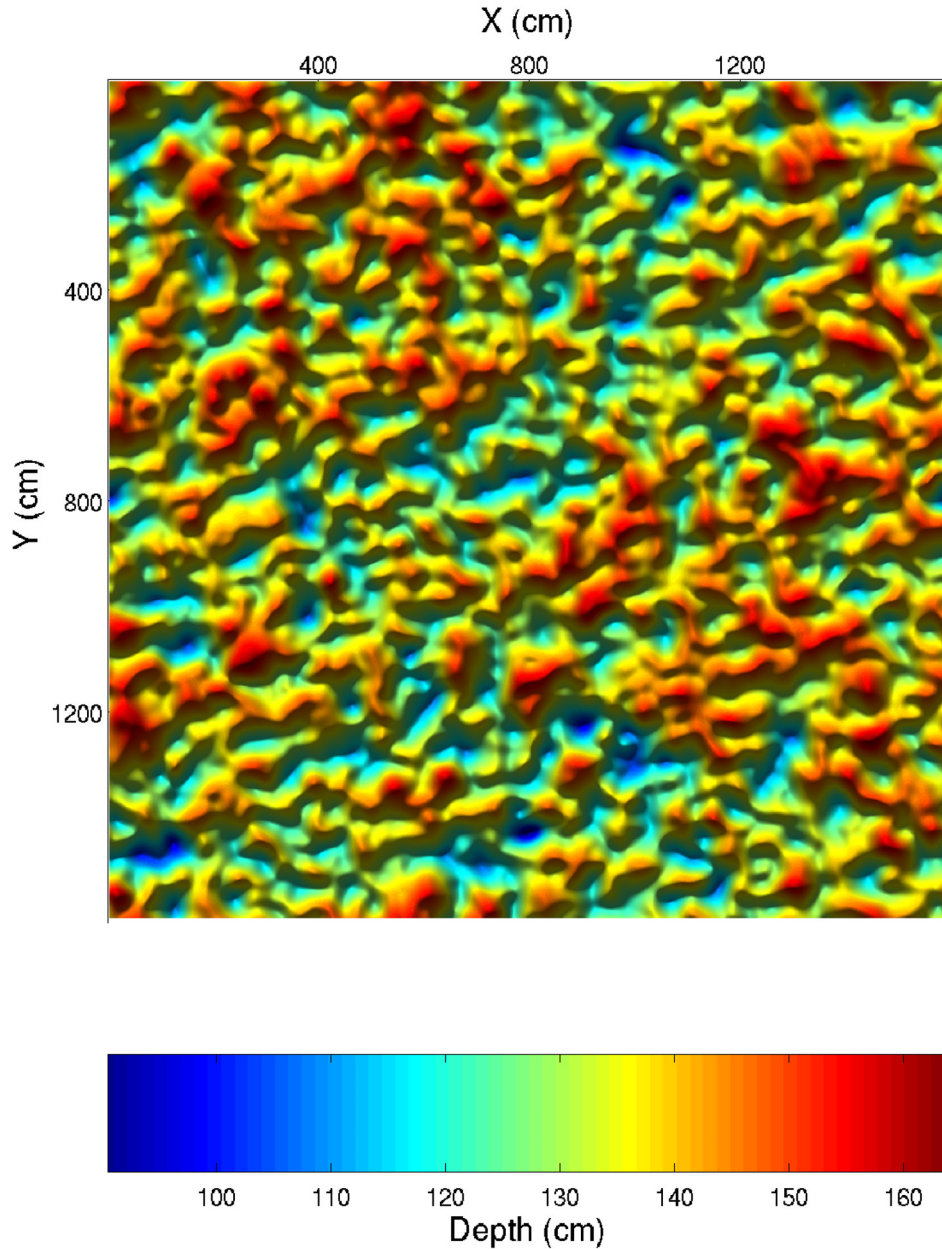


Figure 4. Small-scale topography of a smoothed section of the CMB which covers a surface of 256 m^2 . Computations are made in a regular rectangular parallelepiped mesh of $L \times L \times H$ cells with $L = 1600$ and $H = 200$. The depth is measured from the upper limit of this computation grid.

where

$$\bar{h}_s(t) = \frac{\sum_{i=1}^L \sum_{j=1}^L h_s(i, j, t)}{L^2}$$

and L is, in cell side units, the length of the side of the square over which the topography has been computed. Starting from a flat interface with $L = 1.6 \cdot 10^3$, Figure 4 represents a smoothed version of the small-scale topography obtained 400 years later at the surface of the CMB. This example shows that coupled with diffusion, dissolution and crystallization processes lead to a rough surface over which bumps and holes occur on a wide range of spatial scales. In order to describe in another way such an irregular shape, Figure 5

shows the evolution of the roughness $R_u(t)$ over the last 30 years. Given the permanent fluctuation of the topography, there is no stable state, and the plateau observed at the end of the computation is not the upper limit of the roughness. Nevertheless, the short-scale topography reaches already a vertical extent of $\sim 1 \text{ m}$, which is larger than the thickness of the thermal and Ekman boundary layers [Narteau *et al.*, 2001]. Longer computations in two dimensions show that although some kind of statistical mean value of R_u can be reached, extreme values are more likely to occur.

5. Dissipation on the Small-Scale Topography

[20] Let us then assume that the CMB presents a small-scale topography, or roughness, with the characteristics

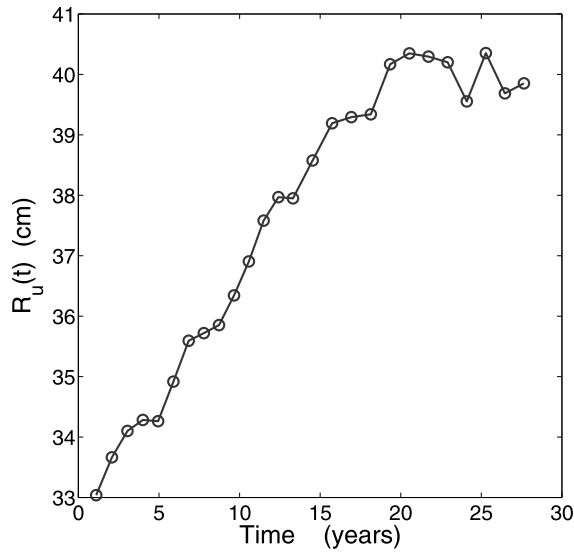


Figure 5. Evolution of the rugosity of the surface of a section of the CMB over 30 years, starting from a flat surface. The small-scale topography at $t = 28$ years is shown in Figure 4.

given in section 4. How much dissipation can be generated by the interaction between this topography and a laminar flow (Poincaré flows, as already said, are nearly rigid body oscillations of the fluid core with respect to the mantle, with a quasi-daily period)? There is no way to compute this interaction in any details; we will just try to get rough orders of magnitude of the dissipated power.

[21] For that, we will first simplify the problem to the extreme. We consider a plane model, which is not a serious limitation. Let $h(x, y)$ be the short-scale topography, and \mathbf{v} be the velocity of the laminar flow beneath the CMB, uniform in the bulk of the fluid (Figure 6). Equivalently, let us consider that the solid half-space with its roughness is moved with respect to the bulk of the fluid with velocity $-\mathbf{v}(t)$; \mathbf{v} is parallel to the x axis in the plane of the mean interface: $\mathbf{v} = v_x \mathbf{x}$. As indicated in section 2,

$$v = v_0 \sin\left(\frac{2\pi}{T}t\right),$$

where $T \approx 24$ hours.

[22] First, we apply the Newton's method to obtain a rough estimate of the possible dissipation. In this approach, after taking a simplified model of the short-scale topography, the interaction between the topography and the fluid is estimated as the energy transfer per unit time necessary to accelerate the liquid from rest up to the velocity of the moving topography. This approximation is justified if the flow is fully turbulent behind the obstacles or if the change in the velocity profile generates waves, which may be dissipated over the entire outer core. In any case this method will give an upper bound for the interaction between the modelled topography and the flow.

[23] Let the velocity at time t be $v(t) > 0$ and consider a domain D of the boundary (CMB). The volume of fluid

which is to be displaced above D , during the time unit, and then accelerated from velocity 0 to velocity v is

$$\dot{V}(t) = v(t) \int_D \mathbf{n} \cdot \mathbf{x} H(\mathbf{n} \cdot \mathbf{x}) dS, \quad (2)$$

where \mathbf{n} is the unit vector normal to the topography, oriented toward the fluid, and H is the Heaviside function. This volume gets the kinetic energy $1/2 \rho v^2$ per unit volume. Let us write that the kinetic energy gained by \dot{V} is equal to the work made in this time unit by the liquid-topography interaction force F_D acting on the portion D of the interface:

$$\frac{1}{2} \rho v^2 \dot{V} = v F_D \quad (3)$$

or

$$F_D = \frac{1}{2} \rho v^2 \int_D \mathbf{n} \cdot \mathbf{x} H(\mathbf{n} \cdot \mathbf{x}) dS. \quad (4)$$

The work of F_D over a period T is

$$W_D = \frac{8}{3\pi} \rho v_0^3 T \int_D \mathbf{n} \cdot \mathbf{x} H(\mathbf{n} \cdot \mathbf{x}) dS. \quad (5)$$

[24] Then, to estimate the integral, we assume (a rough simplification) that the relief is made of regular pyramids with square bases of side A and height h . D being large compared to A^2 , it comes

$$\int_D \mathbf{n} \cdot \mathbf{x} H(\mathbf{n} \cdot \mathbf{x}) dS = \frac{h}{A} S_D,$$

S_D being the area of D . Finally, replacing S_D by the surface of the CMB, we obtain the power given by the interaction force at the CMB:

$$\mathcal{P} = \frac{32}{3} \rho v_0^3 \frac{h}{A} R_c^2, \quad (6)$$

R_c being the core radius.

[25] We compute δ for the case of the retrograde annual nutation, assuming a hydrostatic stratified Earth model (PREM), and we deduce the magnitude of the velocity of

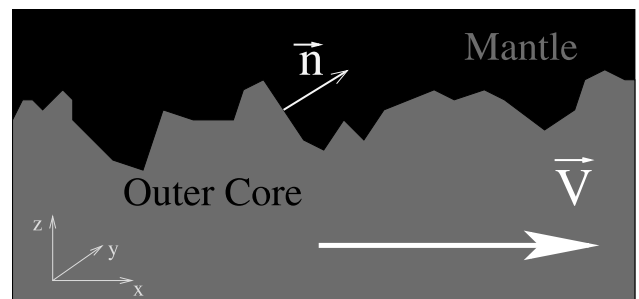


Figure 6. Schematic representation of the CMB on a meter scale. The parameters \mathbf{v} and \mathbf{n} are the velocity of the laminar flow beneath the CMB and the unit vector normal to the topography, respectively.

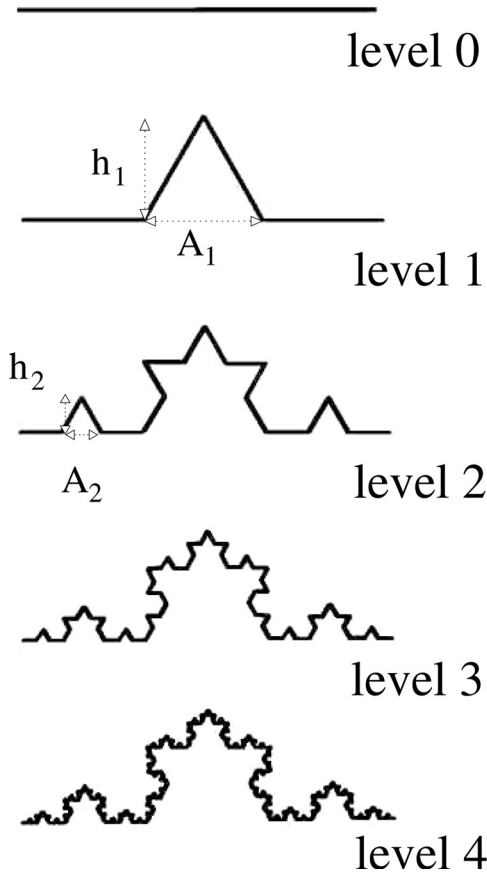


Figure 7. Koch curve at different levels. In this well-known example of a self-similar fractal pattern, the topography appears equally detailed at all scales. Note that the ratio h_i/A_i does not depend on the level i of magnification.

the fluid with respect to the mantle: $v_0 \approx 0.7 \times 10^{-4} \text{ m s}^{-1}$. Taking $h/A = 1$, it comes

$$\mathcal{P} = 5 \times 10^5 \text{ W.}$$

[26] As stressed above, the dissipation problem should also take into account turbulent transport of energy in the outer core, and the Newton's method applied without considering the retroaction of the fluid motion on the boundary behind the obstacles gives an overestimation of the dissipated power. On the contrary, our simplification of the topography in the form of an array of pyramids leads to an underestimation of the effective resistive surface (see section 5).

[27] Let us make another estimate starting with the theory of the motion of ships, which has been the object of a lot of work [e.g., Sedov, 1977]. The determination of the resistance of the ship to the motion relies on the practical possibility to split the resistance into two components, one due to the viscosity, the second one to the ponderability, $W = W_1 + W_2$. The first term is the friction term and writes

$$W_1 = C_f(Re)\rho \frac{Sv^2}{2}, \quad (7)$$

where S is the wet surface of the ship, v is its velocity, ρ the density of water, $Re = UL/\nu$ is the Reynolds number where U is the ship velocity, L a characteristic dimension of the ship and ν is the kinematic viscosity of water. Note that equation (7) comes readily from dimensional analysis. However, the expression of C_f needs more work. It comes [Sedov, 1977]

$$C_f = \frac{0.455}{\log(Re)^{2.58}}.$$

[28] Here, taking again our model of pyramids, we consider that all of them are keels of a multi-keel ship. So we take $L = A \approx 1 \text{ m}$, $U = v$ ($v = v_0 \sin[(2\pi/T)t]$ as before), $\nu = 6 \times 10^{-7} \text{ m}^2 \text{ s}^{-1}$ [Poirier, 2000]. For these values, $C_f \approx 0.07$.

[29] For a given surface of the CMB, S_D , the wet surface is

$$2S_D \sqrt{\frac{1}{4} + \left(\frac{h}{A}\right)^2}.$$

It comes for the dissipated power, following the same computation as before

$$\mathcal{P}_f = \frac{64}{3} C_f(Re)\rho v_0^3 R_c^2 \sqrt{\frac{1}{4} + \left(\frac{h}{A}\right)^2}. \quad (8)$$

[30] For $h/A = 1$, $\mathcal{P}_f \approx 0.15 \mathcal{P}$ (see equation (6)). This is the estimate for smooth pyramids. Adding the short-scale rugosity of our fractal relief, \mathcal{P}_f could be much larger in the same way as when dealing with a ship, “the resistance is much increased when considering rugged keels” [Sedov, 1977, p. 74]; unfortunately, much is not quantified. Let us elaborate on this point. Computing rigorously the interaction of the moving fluid with our fractal relief is out of reach, as already said. We saw that with the regular pyramids model, \mathcal{P}_f depends on the ratio h/A . Instead of considering a single scale pyramids, we can consider the superposition of pyramids of different scales $k \in [1, 2, \dots, K]$ with constant aspect ratio h/A and $h_{k-1}/h_k = R$ (see the Koch curve on Figure 7, where $R = 3$). The friction coefficient and \mathcal{P}_f would be expected to be multiplied by the number K of scales. Of course, there is a limit for K beyond which the reasoning is no longer valid, which may be when h_k is of the order of δ , the thickness of the Ekman layer computed with the value of the molecular viscosity. Again, this simple model does not exhaust the complexity of the reliefs of Figure 4. Of course, all of this amounts to take a larger value of C_f . Taking directly $C_f = 1.33$, apparently a maximum for values found in literature in the case of smoother obstacles, would give $\mathcal{P}_f \sim 1.5 \times 10^6 \text{ W}$. So, friction on a small-scale topography might contribute for an amount of 10^6 W , or even more, to the $4.7 \times 10^6 \text{ W}$ required by astronomical observations [Mathews et al., 2002].

6. Discussion and Conclusion

[31] The above estimate of the dissipated power through friction on a small-scale topography is crude. An approxi-

mation of the relief in the form of a regular pavement of square pyramids makes the free parameter h/A appear, the aspect ratio of the pyramids. That allows an estimate of the effect of more intricate topographies, closer to the ones computed in section 4. The contribution of this mechanism to the dissipation at the CMB could be significant in the case of the annual retrograde nutation, as large as the ohmic dissipation in the high-conductivity model advocated by Buffett *et al.* [2002], possibly larger but probably not big enough by itself

[32] We consider that the power approximated through equations (6) and (8) is entirely dissipated, however, not necessarily in a close vicinity of the CMB. Such a situation is well known in meteorology, when studying the interaction of wind and Earth's surface relief. Recently, it was discovered that the motion of the deep ocean water on the sea bottom irregular topography contributed strongly to the tidal dissipation and that the perturbations of the flow generated by this relative motion could be observed at the ocean surface [Le Provost and Lyard, 1997; Egbert and Ray, 2000].

[33] If it appears that friction on CMB roughness could provide a significant amount of dissipation, it should not either provide a much bigger one, which could conversely put some constraints on the topography parameters. The discussion and statements of Buffett *et al.* [2002] hold indeed in the same terms, whether we get the required dissipative power calling for CMB roughness or for electromagnetic friction (with an enhanced conductivity in the mantle and an enhanced energy of the magnetic field in the vicinity of the CMB). Let us point out that the topography was computed by Narteau *et al.* [2001] without any consideration of the friction problem.

[34] Of course, roughness friction also holds for precession (κ_1). To account for his observations of late Precambrian glaciogenic sequences, Williams [1993] assumed a big change in Earth's obliquity in the 650–430 Ma time interval, from 60° to 26° . This change was attributed to dissipative core-mantle coupling, a mechanism first suggested by Aoki [1969]. However, Pais *et al.* [1999] argued that the viscous and electromagnetic torques, even with the high conductivity model, fail by 4 orders of magnitude to account for such a large change of obliquity. Furthermore, as first shown by Néron de Surgy and Laskar [1997], a big change in obliquity would be accompanied by a big change in the length of the day, which is not observed. Friction on small-scale topography does not bring anything new to this problem.

[35] Another flow exists in the core, responsible for the dynamo action and for the observed secular variation of the geomagnetic field. The effect of this flow on Earth's rotation has been the object of quite a lot of work [e.g., Jault and Le Mouél, 1990; Hinderer *et al.*, 1990; Jault and Le Mouél, 1993; Jackson *et al.*, 1993; Holme, 1998; Holme and de Viron, 2005]. The influence of a CMB small-scale topography on the core-mantle coupling should be also considered in the case of this main flow, although it seems small at first sight. Furthermore, the configuration of this flow in the vicinity of the CMB might be less simple than the Poincaré flow one.

[36] **Acknowledgments.** We thank an unknown referee for helpful remarks and suggestions. We also thank Eduardo Sepúlveda and Olivier

Rozier for their help in computing the CMB topography. This work was supported by 12975-E2C2, a Specific Targeted Research Project of the European Community. At the IPGP, Clément Narteau benefited from a Marie Curie reintegration grant 510640-EVOROCK of the European Community.

References

- Aoki, S. (1969), Friction between mantle and core of the earth as a cause of the secular change in obliquity, *Astron. J.*, *74*, 284–291.
- Bretagnon, P., and N. Capitaine (1997), Précession-nutation, in *Introduction aux Éphémérides Astronomiques*, edited by J.-L. Simon, M. Chapront-Touzé, B. Morando, and W. Thuillot, pp. 117–141, Ed. Phys., Les Ulis, France.
- Buffett, B. A. (1992), Constraints on magnetic energy and mantle conductivity from the forced nutation of the Earth, *J. Geophys. Res.*, *97*, 19,581–19,597.
- Buffett, B. A., E. J. Garnero, and R. Jeanloz (2000), Sediments at the top of the Earth's core, *Science*, *290*, 1338–1342.
- Buffett, B. A., P. M. Mathews, and T. A. Herring (2002), Modeling of nutation and precession: Effects of electromagnetic coupling, *J. Geophys. Res.*, *107*(B4), 2070, doi:10.1029/2000JB000056.
- Busse, F. H. (1968), Steady fluid flow in a precessing spheroidal shell, *J. Fluid Mech.*, *33*, 739–751.
- Egbert, G., and R. Ray (2000), Significant dissipation of tidal energy in the deep ocean inferred from satellite altimeter data, *Nature*, *405*, 775–778.
- Greff, M. (2004), La terre, une toupie au coeur liquide, *Pour Sci.*, *318*, 62–67.
- Greff-Leffitz, M., and H. Legros (1999), Correlation between some major geological events and resonances between the free core nutation and lunisolar tidal waves, *Geophys. J. Int.*, *139*, 131–151.
- Herring, T. A., P. M. Mathews, and B. A. Buffett (2002), Modeling of nutation-precession: Very long baseline interferometry results, *J. Geophys. Res.*, *107*(B4), 2069, doi:10.1029/2001JB000165.
- Hinderer, J., H. Legros, D. Jault, and J.-L. Le Mouél (1990), Core-mantle topographic torque: A spherical harmonic approach and implications for the excitation of the Earth's rotation by core motions, *Phys. Earth Planet. Inter.*, *59*, 329–340.
- Holme, R. (1998), Electromagnetic core-mantle coupling—1. Explaining decadal changes in the length of day, *Geophys. J. Int.*, *132*, 167–180.
- Holme, R., and O. de Viron (2005), Geomagnetic jerks and a high-resolution length-of-day profile for core studies, *Geophys. J. Int.*, *160*, 435–439, doi:10.1111/j.1365-246X.2004.02510.x GJI.
- Jackson, A., J. Bloxham, and D. Gubbins (1993), Time-dependent flow at the core surface and conservation of angular momentum in the coupled core–mantle system, in *Dynamics of the Earth's Deep Interior and Earth Rotation*, *Geophys. Monogr. Ser.*, vol. 72, J.-L. Mouél, D. E. Smylie, and T. Herring, pp. 97–107, AGU, Washington, D. C.
- Jault, D., and J.-L. Le Mouél (1990), Core–mantle boundary shape: Constraints inferred from the pressure torque acting between the core and the mantle, *Geophys. J. Int.*, *101*, 233–241.
- Jault, D., and J.-L. Le Mouél (1993), Circulation in the liquid core and coupling with the mantle, *Adv. Space Res.*, *13*, 221–233.
- Kerswell, R. R. (1993), The instability of precessing flows, *Geophys. Astrophys. Fluid Dyn.*, *72*, 107–144.
- Knittle, E., and R. Jeanloz (1989), Simulating the core-mantle boundary: An experimental study of high-pressure reactions between silicates and liquid iron, *Geophys. Res. Lett.*, *16*, 609–612.
- Le Mouél, J.-L., G. Hulot, and J.-P. Poirier (1997), Core-mantle interactions, in *Earth's Deep Interior*, edited by D. Crossley, pp. 197–221, Gordon and Breach, New York.
- Le Provost, C., and L. Lyard (1997), Energetics of the barotropic ocean tides: An estimate of bottom friction dissipation from hydrodynamic model, *Prog. Oceanogr.*, *40*, 37–52.
- Loper, D. E. (1975), Torque balance and energy budget for the precessionally driven dynamo, *Phys. Earth Planet. Inter.*, *11*, 43–60.
- MacDonald, J. F., and N. F. Ness (1961), A study of free oscillations of the Earth, *J. Geophys. Res.*, *66*, 1865–1911.
- Mathews, P. M., T. A. Herring, and B. A. Buffett (2002), Modeling of nutation and precession: New nutation series for nonrigid Earth and insights into the Earth's interior, *J. Geophys. Res.*, *107*(B4), 2068, doi:10.1029/2001JB000390.
- Narteau, C., J.-L. Le Mouél, J. Poirier, E. Sepúlveda, and M. G. Shnirman (2001), On a small scale roughness of the core-mantle boundary, *Phys. Earth Planet. Inter.*, *191*, 49–61.
- Néron de Surgy, O., and J. Laskar (1997), On the long term evolution of the spin of the Earth, *Astron. Astrophys.*, *318*, 975–989.
- Noir, J., D. Jault, and P. Cardin (2001), Numerical study of the motions within a slowly precessing sphere, at low Ekman number, *J. Fluid Mech.*, *437*, 283–299.

- Pais, M. A., and J.-L. Le Mouël (2001), Precession-induced flows in liquid-filled containers and in the Earth's core, *Geophys. J. Int.*, *144*, 539–554.
- Pais, M. A., J.-L. Le Mouël, K. Lambeck, and J. Poirier (1999), Late Precambrian paradoxical glaciation and obliquity of the Earth—A discussion of dynamical constraints, *Earth Planet. Sci. Lett.*, *174*, 155–171.
- Poincaré, R. (1910), Sur la précession des corps déformables, *Bull. Astron.*, *27*, 321–356.
- Poirier, J. P. (2000), *Introduction to Physics of the Earth's Interior*, Cambridge Univ. Press, New York.
- Poirier, J. P., and J. L. Le Mouël (1992), Does infiltration of core material into the lower mantle affect the observed geomagnetic field?, *Phys. Earth Planet. Inter.*, *73*, 29–37.
- Poirier, J. P., V. Malavergne, and J.-L. Le Mouël (1998), Is there a thin electrically conducting layer at the base of the mantle?, in *The Core-Mantle Boundary Region, Geodyn. Ser.*, vol. 28, edited by M. Gurnis et al., pp. 131–137, AGU, Washington, D. C.
- Roberts, P. H. (1965), On the thermal instability of a highly rotating fluid sphere, *Astrophys. J.*, *141*, 240–250.
- Roberts, P. H., and K. Stewartson (1965), On the motion of a liquid in a spheroidal cavity of a precessing rigid body—ii, *Proc. Cambridge Philos. Soc.*, *61*, 279–288.
- Rochester, M. (1976), The secular decrease of obliquity due to dissipative core-mantle coupling, *Geophys. J. R. Astron.*, *46*.
- Sasao, T., I. Okamoto, and S. Sakai (1997), Dissipative core-mantle coupling and nutational motion of the Earth, *Publ. Astron. Soc. Jpn.*, *29*, 83–105.
- Sedov, L. (1977), *Similitudes et Dimensions en Mécanique*, Mir, Moscow.
- Shankland, T. J., J. Peyronneau, and J. Poirier (1993), Electrical conductivity of the Earth's lower mantle, *Nature*, *366*, 453–455.
- Stacey, F. D. (1973), The coupling of the core to the precession of the Earth, *Geophys. J. R. Astron. Soc.*, *33*, 47–55.
- Stewartson, K., and P. H. Roberts (1963), On the motion of a liquid in a spheroidal cavity of a precessing rigid body, *J. Fluid Mech.*, *17*, 1–20.
- Tilgner, A. (1999), Magnetohydrodynamic flow in precessing fluid spherical shells, *J. Fluid Mech.*, *379*, 303–318.
- Toomre, A. (1974), On the 'nearly diurnal wobble' of the Earth, *J. Fluid Mech.*, *38*, 335–348.
- Vanyo, J., P. Wilde, P. Cardin, and P. Olson (1995), Experiments on precessing flows in the Earth's liquid core, *Geophys. J. Int.*, *121*, 136–142.
- Vanyo, J. P. (1991), A geodynamo powered by luni-solar precession, *Geophys. Astrophys. Fluid Dyn.*, *59*, 209–234.
- Williams, G. E. (1993), History of the Earth's obliquity, *Earth Sci. Rev.*, *112*, 1–45.

M. Greff-Lefftz and J. L. Le Mouël, Laboratoire de Géomagnétisme, Institut de Physique du Globe de Paris, 4, Place Jussieu, Paris, Cedex 05, F-75252, France. (greff@ipgp.jussieu.fr; lemouel@ipgp.jussieu.fr)

M. Holschneider, Institute of Applied and Industrial Mathematics, Universität Potsdam, POB 601553, D-14115 Potsdam, Germany. (hols@math.uni-potsdam.de)

C. Narteau, Laboratoire de Dynamique des Systèmes Géologiques, Institut de Physique du Globe de Paris, 4, Place Jussieu, Paris, Cedex 05, F-75252, France. (narteau@ipgp.jussieu.fr)